

Low-Rank Spatial Channel Estimation for Millimeter Wave Cellular Systems

Parisa A. Eliasi, *Student Member, IEEE*, Sundeep Rangan, *Senior Member, IEEE*,
Theodore S. Rappaport, *Fellow, IEEE*

Abstract—The tremendous bandwidth available in the millimeter wave (mmW) frequencies between 30 and 300 GHz have made these bands an attractive candidate for next-generation cellular systems. However, reliable communication at these frequencies depends extensively on beamforming with very high-dimensional antenna arrays. Estimating the channel sufficiently accurately to perform beamforming can thus be challenging both due to low coherence time and large number of antennas. Also, the measurements used for channel estimation may need to be made with analog beamforming where the receiver can “look” in only one direction at a time. This work presents a novel method for estimation of the receive-side spatial covariance matrix of a channel from a sequence of power measurements made at different angular directions. The method reduces the spatial covariance estimation to a matrix completion optimization problem. To reduce the number of measurements, the optimization can incorporate the low-rank constraints in the channels that are typical in the mmW setting. The optimization is convex and fast, iterative methods are presented to solving the problem. Simulations are presented for both single and multi-path channels using channel models derived from real measurements in New York City at 28 GHz..

I. INTRODUCTION

Meeting the tremendous growth in demand for cellular data [1] will require new technologies that can provide orders of magnitude increases in wide-area wireless capacity. With the severe shortage of spectrum in traditional UHF and microwave bands below 3 GHz, there has been considerable interest in so-called millimeter wave (mmW) frequencies between 30 and 300 GHz where vast amounts of essentially virgin spectrum are still widely available [2]–[7].

However, a significant challenge for using mmW for wide-area, cellular-type coverage is range. Due to Friis’ Law [8], the high frequencies of mmW signals result in large isotropic path loss. Fortunately, the very small wavelengths of mmW signals combined with advances in low-power CMOS RF circuits enable large numbers (≥ 32 elements) of miniaturized antennas to be placed in small dimensions thereby providing high beamforming gains that can theoretically more than compensate for the increase in isotropic path loss [9].

However, spatial channel estimation needed to support beamforming presents several challenges in the mmW range:

- *High-dimensional arrays:* Since current mobile devices typically have one to four antennas, the array sizes in the mmW range – which may be 16 or 32 elements even at the mobile – will represent a significant increase in the dimension of the antenna processing. In particular, a much larger number of parameters will need to be tracked at the receiver for channel estimation. A system with N_{rx} receive antennas must estimate N_{rx} channels per transmit stream for instantaneous beamforming and N_{rx}^2 parameters for the receive-side spatial covariance matrix used in long-term beamforming.
- *Rapid channel variations:* The high frequencies of the mmW bands implies that the coherence time of the channel may be very small, meaning that each of the channels to be tracked can be varying rapidly. Channel tracking for small-scale fading can be avoided by long-term beamforming [10], and simulations based on experimental measurements in [9] suggest that the long-term beamforming introduces only a 1 to 2 dB loss in the mmW range. However, since mmW signals are extremely susceptible to blocking [7], even the large-scale channel characteristics may change rapidly. For example, a change in the orientation of the mobile device, movement of a hand holding the device or appearance of a wall would all change the channel significantly. Thus, channel statistics must be estimated with a limited number of measurements.
- *Analog beamforming:* Due to the high bandwidths and large number of antenna elements in the mmW range, it may not be possible from a power consumption perspective for the mobile receiver to obtain high rate digital samples from all antenna elements [11]. Most proposed designs perform beamforming in analog (either in RF or IF) prior to the A/D conversion [12]–[15] – see Fig. 1. A key limitation for these architectures is that they permit the mobile to “look” in only one or a small number of directions at a time. This feature significantly reduces the information in each measurement, further complicating the channel estimation process.

In this paper, we consider the problem of estimating the long-term receive-side spatial covariance of a channel on a high-dimensional array from a limited number of analog measurements. Key to our methodology is that the mmW channels will likely have a low-rank structure relative to the number of antenna elements. For example, extensive measurements at

This material is based upon work supported by the National Science Foundation under Grants No. 1116589 and 1237821 as well as generous support from Samsung, Nokia Siemens Networks, Intel, Qualcomm and InterDigital Communications.

The authors are with NYU WIRELESS, New York University Polytechnic School of Engineering, Brooklyn, NY 11201 USA (e-mail: pa854@nyu.edu; srangan@nyu.edu; tsr@nyu.edu).

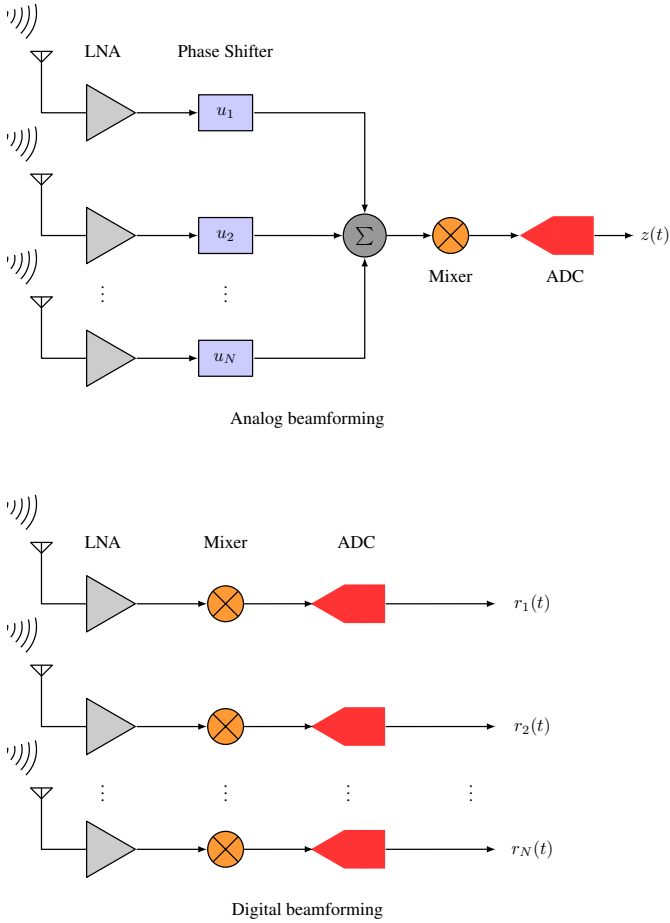


Fig. 1: Analog vs. digital beamforming. Bottom panel: Front-ends at conventional frequencies typically digitize the signals from each antenna separately. This fully digital architecture offers the greatest flexibility. However, power consumption may be prohibitive in the mmW range when the bandwidth and number of antennas is large. **Top panel:** To reduce power consumption, mmW front-end receivers may need to perform beamforming in analog via phase shifters. A consequence of this architecture for channel estimation is that each measurement provides information in only one direction at a time.

28 and 73 GHz in New York City [4], [16], [17] – a dense, urban environment similar to likely initial deployments for mmW systems – have shown that the mmW channel energy is often concentrated in a small number of relatively narrow-beam clusters. Analysis of this data in [9] have revealed that the channel is often well approximated by a rank three or four channel, typically much smaller than the antenna dimension. Similar findings can be found in [18]. This low-rank property implies that the spatial covariance matrix can be characterized by a relatively small number of parameters for the purpose of channel estimation.

Of course, the use of low-rank spatial structure is widely-used in array processing and underlies many classic channel estimation for wireless systems [19]–[21]. The contribution in this work is to consider the use of low-rank channel

estimation from analog measurements. As we describe below, each measurement from an array with analog phase shifting provides a power measurement in a single angular direction. We show that maximum likelihood (ML) reconstruction of the channel covariance matrix from a collection of such measurements made at random angles is similar to a low-rank matrix completion problem that has been used widely in machine learning and image processing.

There are now several algorithms to solve low-rank matrix reconstruction — most are either based on nuclear or trace norm regularization [22]–[24] or message passing techniques [25], [26]. A recent work [27] has also considered low-rank recovery problem specifically for covariance matrix estimation. In this paper, we adapt a simple iterative soft thresholding algorithm (ISTA) method [28] originally used in sparse recovery problems, but also used for matrix completion [29]. The method here is modified to account for the non-Gaussian nature of the power measurements in the ML objective. It is shown that the proposed ISTA-based algorithm converges to the global maxima of the likelihood.

Unfortunately, similar to the original work [29], the thresholding step in each iteration of the proposed ISTA method requires an eigenvalue decomposition of the current covariance matrix estimate. This computation may preclude implementation for real-time system. We thus propose an alternate approximate ML estimate, where the search is performed over an appropriately chosen finite subspace. We show that the resulting optimization for the approximate ML estimate is equivalent to an inference problem for a generalized linear model (GLM) [30] with non-negative components. An similar ISTA method can be used to solve this GLM-type optimization, using simple scalar thresholding avoiding all eigenvalue decompositions.

Both the exact and approximate ML algorithms are tested in both single-path and multi-path models. The channels for the multipath test scenarios are from [9] based on 28 GHz New York City data mentioned above [4], [16], [17], [31]. It is shown that the exact ML method offers excellent performance in a relatively small number of iterations and the approximate ML method is only slightly worse.

II. PROBLEM FORMULATION

The problem is to estimate the second-order spatial statistics between a transmitter (TX) and receiver (RX). We assume that the TX sends data from a single antenna, or equivalently, from multiple TX antennas with a fixed beamforming vectors. The RX has N antennas, and makes L measurements. In each measurement ℓ , $\ell = 1, \dots, L$, the TX sends D waveforms, $p_{\ell d}(t)$, $d = 1, \dots, D$, potentially at the same time, but at different frequencies.

An example transmission scheme is illustrated in Fig. 2. In this example, the transmissions are separated in time as would occur for periodic synchronization signals such as those proposed for the Primary Synchronization Signal in [32]. However, the method proposed here would equally apply to

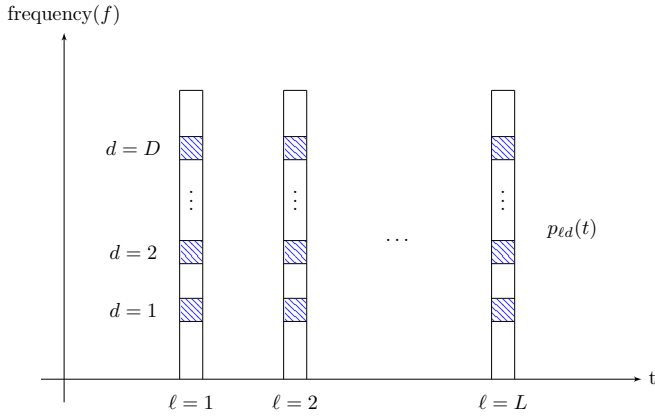


Fig. 2: Model for the synchronization signals from which the spatial channel must be estimated. The signal is transmitted L time slots, and, for frequency diversity, the signal may be transmitted in D different frequencies in each time slot. We will evaluate the estimation performance as a function of D and L .

measurements from a continuous sequence of time slots such as cell reference signals.

We assume the received complex baseband signal across the N antenna from the transmission is given by the vector $\mathbf{r}_\ell(t) \in \mathbb{C}^N$, where

$$\mathbf{r}_\ell(t) = \frac{1}{\sqrt{D}} \sum_{d=1}^D \mathbf{h}_{\ell d} p_{\ell d}(t) + \mathbf{v}_\ell(t), \quad (1)$$

where $\mathbf{h}_{\ell d}$ is the channel gain vector for the signal $p_{\ell d}(t)$ and $\mathbf{v}_\ell(t)$ is complex AWGN with noise PSD N_0 Watts/Hz. Implicitly, we assume in this model that each $p_{\ell d}(t)$ is transmitted in a sufficiently small time and frequency region that the channel is flat across the transmission. The factor $1/\sqrt{D}$ is used to normalized the power.

We will assume a standard *correlated Rayleigh fading model* [33], where the instantaneous channel gains $\mathbf{h}_{\ell d}$ have complex Gaussian distributions

$$\mathbf{h}_{\ell d} \sim \mathcal{CN}(0, \mathbf{Q}), \quad \mathbf{Q} = \mathbb{E}(\mathbf{h}_{\ell d} \mathbf{h}_{\ell d}^*), \quad (2)$$

for some spatial covariance matrix \mathbf{Q} . In addition, we will assume that in each measurement ℓ , the channel is independently faded across the different transmissions, $\mathbf{h}_{\ell d}$, $d = 1, \dots, D$. We thus call the parameter D the *diversity order*.

In this paper, we do not consider the problem of predicting the *instantaneous* channel gains $\mathbf{h}_{\ell d}$. Instantaneous channel tracking across a large number of antennas may be difficult in the mmW regime due to the low coherence time and the limitation that the channel can be observed in only direction at a time due to analog beamforming [5], [7]. Instead, in this paper, we thus consider only the problem of tracking the second-order spatial statistics, namely the matrix \mathbf{Q} . As described in [33], the covariance matrix \mathbf{Q} is determined by the angles of arrivals of different paths from the transmitter, their relative average powers and the response of the receive antenna array to the each of these paths. Unlike the instantaneous channel gains

$\mathbf{h}_{\ell d}$ which will vary due to small scale motion (on the order of a wavelength), the long-term statistics such as \mathbf{Q} depend only on the macro-layer scattering environment and are thus a relatively constant over much longer periods of time and frequency. In particular, in this study, we will assume that \mathbf{Q} is constant over all measurements $\ell = 1, \dots, L$.

Once the spatial covariance matrix is estimated, one can perform a number of long-term beamforming techniques [10]. For example, the long-term beamforming vector that maximizes the average signal energy can be determined from the maximal eigenvector of \mathbf{Q} . Similarly, if one estimates spatial covariance matrix \mathbf{Q}_{sig} of a desired signal and the covariance matrix \mathbf{Q}_{int} of the interference plus noise, the maximal eigenvector of $\mathbf{Q}_{int}^{-1/2} \mathbf{Q}_{sig} \mathbf{Q}_{int}^{-1/2}$ is the direction that maximizes the signal-to-interference plus noise (SINR). As mentioned in the Introduction, simulations in [9] suggest that the loss from optimal long-term beamforming in the mmW range relative to instantaneous beamforming is on the order of 1 dB.

In estimating the spatial covariance matrix \mathbf{Q} , our key problem assumption is that the RX does not have direct digital samples of the components of the vector $\mathbf{r}_\ell(t)$ from the different antennas. Instead, in each measurement ℓ , the RX must apply some beamforming vector $\mathbf{u}_\ell \in \mathbb{C}^N$ in analog and then perform the estimation from the weighted signal $\mathbf{u}_\ell^* \mathbf{r}_\ell(t)$. To perform the estimation, we assume that the RX performs a match filter with each of the signals $p_{\ell d}(t)$ to yield complex scalar outputs,

$$z_{\ell d} = \frac{1}{\sqrt{E_s} \|\mathbf{u}_\ell\|} \int p_{\ell d}^*(t) \mathbf{u}_\ell^* \mathbf{r}_\ell(t) dt, \quad E_s = \int |p_{\ell d}(t)|^2 dt \quad (3)$$

where E_s is the energy in the transmitted signal. We assume that E_s is the same for all $p_{\ell d}(t)$.

III. MAXIMUM LIKELIHOOD ESTIMATION AND MATRIX COMPLETION

A. Maximum Likelihood Estimation

The problem is to estimate the spatial covariance matrix \mathbf{Q} from the measurements $z_{\ell d}$. We will assume that noise level N_0 is known. We will also assume that the signals $p_{\ell d}(t)$ are orthogonal, and the channel gains $\mathbf{h}_{\ell d}$ are independently faded across ℓ and d and independent of the noise $\mathbf{v}(t)$. Under these assumptions, it can be verified that the accumulated energies

$$y_\ell = \sum_{d=1}^D |z_{\ell d}|^2, \quad (4)$$

provide a sufficient statistic for the unknown parameters \mathbf{Q} and N_0 . Moreover, under the independence assumptions, the random variables y_ℓ will be distributed as

$$Y_\ell = \frac{\lambda_\ell}{2D} V_\ell,$$

where V_ℓ is a chi-squared random variable with $2D$ degrees of freedom, and λ_ℓ is the energy

$$\lambda_\ell(\mathbf{Q}) = \mathbf{u}_\ell^* [\mathbf{Q} + \gamma^{-1} \mathbf{I}] \mathbf{u}_\ell, \quad \gamma = \frac{E_s}{N_0}. \quad (5)$$

See similar calculations in [34]. If we let $\mathbf{y} = (y_1, \dots, y_L)$ be the vector of the received powers in the L measurements. then the negative log likelihood of \mathbf{y} given \mathbf{Q} is

$$-\log p(\mathbf{y}|\mathbf{Q}) = C + \sum_{\ell=1}^L \left[D \log(\lambda_\ell(\mathbf{Q})) + \frac{Dy_\ell}{\lambda_\ell(\mathbf{Q})} \right], \quad (6)$$

where $\lambda_\ell(\mathbf{Q})$ is given in (5) and C is some constant that does not depend on \mathbf{Q} (although it may depend on \mathbf{y}). Thus, we have the ML estimation of \mathbf{Q} is given by

$$\hat{\mathbf{Q}} = \arg \min_{\mathbf{Q}} J(\mathbf{Q}) \text{ s.t. } \mathbf{Q} \geq \mathbf{0}, \quad (7)$$

where

$$J(\mathbf{Q}) := \sum_{\ell=1}^L \left[\log(\lambda_\ell(\mathbf{Q})) + \frac{y_\ell}{\lambda_\ell(\mathbf{Q})} \right]. \quad (8)$$

B. Connections to Matrix Completion

An arbitrary $N \times N$ matrix \mathbf{Q} has N^2 unknowns, and a Hermetian matrix $\mathbf{Q} = \mathbf{Q}^*$ has $N(N+1)/2$ unknowns. Thus, one may think that one would need at least $L \geq N(N+1)/2$ measurements to fully reconstruct \mathbf{Q} . However, a key property of the covariance matrix \mathbf{Q} in the mmW range is that it is typically ‘‘almost’’ low-rank, meaning that the most of the energy of the channel gains $\mathbf{h}_{\ell d}$ is concentrated in a low-dimensional subspace. For wireless channels, the rank of the receive-side spatial covariance matrix \mathbf{Q} is determined by the number of distinct angles of arrival of paths from the transmitter [33]. In the mmW range, analysis in [9] of the 28 and 73 GHz measurements in New York City in [4], [16], [17], [31], revealed that when low-power transmitters were placed in microcellular type deployments, receivers in most street-level locations saw only two to three dominant path clusters, each with a relatively small angular spread. The clustering of the paths into small, relatively narrowbeam clusters causes the spatial covariance matrix to be low-rank. For example, simulations in [9] assuming a 4x4 uniform linear array with the NYC channels showed that, most of the energy would be likely concentrated to three to four-dimensional space – much lower than the 16 dimensions of the antenna array.

This low-rank property can be exploited to recover the matrix \mathbf{Q} from less than N^2 measurements. To understand how this is possible, consider the problem of low-rank matrix completion used in machine vision and ranking systems [22]–[24]. In the matrix completion problem, one is to reconstruct a low-rank matrix \mathbf{A} from a small number of entries A_{ij} . If an $M \times N$ matrix \mathbf{A} has rank r , it has only $O(r(M+N))$ degrees of freedom. When the rank r is small, this number of degrees of freedom may be significantly less than the MN parameters needed to describe a general matrix. Low-rank matrix completion methods impose the low-rank rank constraint

In the ML estimation problem considered here, each measurement y_ℓ in (5) has an average value λ_ℓ in (5) which is a linear function of the unknown matrix \mathbf{Q} . Hence, the ML estimation problem can be considered a ‘‘noisy’’ matrix completion problem where we attempt to attempt to

reconstruct a matrix an $N \times N$ low-rank matrix \mathbf{Q} from L noisy linear measurements of \mathbf{Q} . The difference between the ML estimation problem considered here in contrast to the estimation problems here

C. Sparsity Regularization

Placing a low-rank constraint on \mathbf{Q} in the optimization (7) will, in general, result in a non-convex optimization. Most matrix completion methods such as [22]–[24] thus impose the low-rank constraint indirectly by adding a regularization term of the form $\|\mathbf{Q}\|_*$ to the objective where $\|\mathbf{Q}\|_*$ is the so-called nuclear norm, which is the sum of the singular values of \mathbf{Q} . In our problem, the matrix \mathbf{Q} is positive semi-definite, so the nuclear norm is simply the trace: $\|\mathbf{Q}\|_* = \text{Tr}(\mathbf{Q})$. We thus consider the regularized optimization

$$\hat{\mathbf{Q}} = \arg \min_{\mathbf{Q}} J_\mu(\mathbf{Q}) \text{ s.t. } \mathbf{Q} \geq \mathbf{0}, \quad (9)$$

where

$$J_\mu(\mathbf{Q}) := J(\mathbf{Q}) + \mu \text{Tr}(\mathbf{Q}), \quad (10)$$

and $\mu > 0$ is a regularization parameter. When $\mu = 0$, the objective function (10) agrees with the original un-regularized ML objective (8). Using $\mu > 0$ tends to enforce the requirement that \mathbf{Q} is lower rank by penalizing the eigenvalues of \mathbf{Q} . In analogy with compressed sensing, the parameter $\mu > 0$ is often considered a *sparsity* regularizer since the resulting eigenvalues of the optimal solution $\hat{\mathbf{Q}}$ in (9) tend to have a sparse set of eigenvalues, meaning that many will be zero [22]–[24].

Interestingly, in the simulations below, we will see that $\mu > 0$ appears to not improve the performance over $\mu = 0$. This phenomena is significantly different than the standard matrix completion problem where using $\mu > 0$ is essential. However, the ML objective (7) already imposes a positivity constraint $\mathbf{Q} > 0$. It is known that in related problems [35], that non-negativity constraints already tends to result in sparse solutions with many zero values – so it is not surprising that using $\mu > 0$ does not help.

IV. OPTIMIZATION METHODS

A. ISTA Algorithm

The objective function $J(\mathbf{Q})$ in (8) in the optimization (7), or the sparsity-regularized version $J_\mu(\mathbf{Q})$ in (10), are both convex and therefore can be minimized via a number of methods. We will first consider a simple ISTA approach [28] used commonly in compressed sensing. We will describe the ISTA algorithm for the sparsity-regularized objective function $J_\mu(\mathbf{Q})$ in (10). The algorithm for minimizing $J(\mathbf{Q})$ can be realized by taking $\mu = 0$.

For the optimization (9), the ISTA algorithm produces a sequences of estimates \mathbf{Q}_k , $k = 0, 1, 2, \dots$ with updates that can be described as follows: At each iteration k , we find an $\alpha_k > 0$ such that

$$J_\mu(\mathbf{Q}) \leq \bar{J}_\mu(\mathbf{Q}, \mathbf{Q}_k) := J_\mu(\mathbf{Q}_k) + \frac{\partial J_\mu(\mathbf{Q}_k)}{\partial \mathbf{Q}} \cdot (\mathbf{Q} - \mathbf{Q}_k) + \frac{1}{2\alpha_k} \|\mathbf{Q} - \mathbf{Q}_k\|_F^2, \quad (11)$$

for all possible $\mathbf{Q} \geq 0$. We will discuss how to select such a value α_k momentarily. Thus, $\bar{J}_\mu(\mathbf{Q}, \mathbf{Q}_k)$ represents a quadratic upper bound on the true objective $J_\mu(\mathbf{Q})$ that matches the true objective at $\mathbf{Q} = \mathbf{Q}_k$. In the case of the objective function (8), it is easy to check that the derivative in any direction Δ is given by

$$\frac{\partial J_\mu(\mathbf{Q}_k)}{\partial \mathbf{Q}} \cdot \Delta = \text{Tr}(\mathbf{S}_k^* \Delta), \quad (12)$$

where

$$\mathbf{S}_k = \sum_{\ell=1}^L \left[\frac{1}{\lambda_\ell(\mathbf{Q}_k)} - \frac{y_\ell}{\lambda_\ell^2(\mathbf{Q}_k)} \right] \mathbf{u}_\ell \mathbf{u}_\ell^* + \mu \mathbf{I}. \quad (13)$$

The concept in the ISTA algorithm is, at each iteration k , to minimize the upper bound $\bar{J}_\mu(\mathbf{Q}, \mathbf{Q}_k)$ instead of the true objective $J_\mu(\mathbf{Q})$:

$$\begin{aligned} \mathbf{Q}_{k+1} &= \arg \min_{\mathbf{Q} \geq 0} \bar{J}_\mu(\mathbf{Q}, \mathbf{Q}_k) \\ &\stackrel{(a)}{=} \arg \min_{\mathbf{Q} > 0} \text{Tr}(\mathbf{S}_k^* \mathbf{Q}) + \frac{1}{2\alpha_k} \|\mathbf{Q} - \mathbf{Q}_k\|_F^2 \\ &\stackrel{(b)}{=} \arg \min_{\mathbf{Q} \geq 0} \|\mathbf{Q} - \mathbf{Q}_k + \alpha_k \mathbf{S}_k\|_F^2 \\ &\stackrel{(c)}{=} T_+(\mathbf{Q}_k - \alpha_k \mathbf{S}_k), \end{aligned} \quad (14)$$

where in step (a) we substituted the definition of $\bar{J}_\mu(\cdot)$ in (11) and derivative (12) and removed terms that do not depend on \mathbf{Q} ; step (b) follows from rearranging the quadratic and in step (c) the operator $T_+(\mathbf{P})$ is called the *proximal operator* and is given by

$$T_+(\mathbf{P}) := \arg \min_{\mathbf{Q} \geq 0} \|\mathbf{Q} - \mathbf{P}\|_F^2. \quad (15)$$

It is shown in [29] that this minimization can be computed easily via an eigenvalue decomposition. Specifically, when $\mathbf{P} = \mathbf{P}^*$, we know that $\mathbf{P} = \mathbf{U}\mathbf{D}\mathbf{U}^*$ for some unitary \mathbf{U} and real diagonal $\mathbf{D} = \text{diag}(\mathbf{d})$. In this case, the proximal operator is

$$T_+(\mathbf{P}) = \mathbf{U} \text{diag}[\max(\mathbf{d}, 0)] \mathbf{U}^*,$$

which simply thresholds the eigenvalues of the matrix. The resulting algorithm is shown in Algorithm 1.

Algorithm 1 ML Estimation via ISTA

Require: Matrix search directions \mathbf{u}_ℓ , power values y_ℓ , $\ell = 1, \dots, L$, and SNR γ .

- 1: $t \leftarrow 0$
 - 2: Initialize $\mathbf{Q}_0 \geq 0$
 - 3: **repeat**
 - 4: $\lambda_\ell \leftarrow \mathbf{u}_\ell^* (\mathbf{Q}_k + \gamma^{-1} \mathbf{I}) \mathbf{u}_\ell, \forall \ell$
 - 5: Compute the gradient \mathbf{S}_k from (13)
 - 6: Select step size $\alpha_k > 0$
 - 7: $\mathbf{Q}_{k+1} \leftarrow T_+(\mathbf{Q}_k - \alpha_k \mathbf{S}_k)$
 - 8: **until** Terminated
-

A key property of the ISTA algorithm is that the objective function monotonically decreases for a sufficiently small step-size.

Proposition 1: Consider the output of the ISTA algorithm, Algorithm (1), generated for a set of measurement vectors \mathbf{u}_ℓ , power measurements y_ℓ and SNR value $\gamma > 0$. Then, there exists a minimum step size $\bar{\alpha} > 0$ such that if $\alpha_k < \bar{\alpha}$ for all k , the objective $J_\mu(\mathbf{Q})$ monotonically decreases.

Proof: From Taylor's Theorem, we know that the bound (11) will be satisfied if

$$\frac{\partial^2}{\partial \mathbf{Q}^2} J_\mu(\mathbf{Q}) \leq \frac{1}{2\alpha_k} \mathbf{I}. \quad (16)$$

Now, since $\mathbf{Q} \geq \mathbf{0}$, the power levels $\lambda_\ell(\mathbf{Q})$ in (5) will be bounded below by

$$\lambda_\ell(\mathbf{Q}) \geq \frac{\|\mathbf{u}_\ell\|^2}{\gamma}.$$

Using this bound, one can verify that there is a global upper bound on the Hessian in the left-hand side of (16). This implies that there exists an $\bar{\alpha} > 0$ such that if $\alpha_k < \bar{\alpha}$ then (16) will be satisfied and therefore so will the bound (11). We therefore have that at each iteration k ,

$$J_\mu(\mathbf{Q}_{k+1}) \stackrel{(a)}{\leq} \bar{J}_\mu(\mathbf{Q}_{k+1}, \mathbf{Q}_k) \stackrel{(b)}{\leq} \bar{J}_\mu(\mathbf{Q}_k, \mathbf{Q}_k) \stackrel{(c)}{=} J_\mu(\mathbf{Q}_k), \quad (17)$$

where step (a) follows from quadratic upper bound approximation in (11), step (b) is based on monotonically decreasing behavior of the cost function when we are applying ISTA algorithm, and in step (c) we substituted the \mathbf{Q}_k in (11). This shows that for sufficiently small step sizes, the objective function decreases monotonically. ■

A more refined analysis along the lines of [28] will show additionally that the $J_\mu(\mathbf{Q}_k)$ converges to a local minima, which will also be a global minima since the function is convex.

B. Adaptive Step-size Selection

Proposition 1 guarantees that for a sufficiently small step-size $\bar{\alpha}$, the algorithm is guaranteed to converge. However, selecting a single step-size that works for all \mathbf{Q}_k may require a very small value, slowing the rate of the algorithm. We thus use a simple, standard backtracking adaptive step-size method [36] as follows. In each iteration of our algorithm, we attempt a candidate step size $\alpha_k > 0$ and compute a test estimate $\tilde{\mathbf{Q}}_{k+1}$. We know that, from a first-order approximation of the objective,

$$J_\mu(\tilde{\mathbf{Q}}_{k+1}) \approx J_\mu(\mathbf{Q}_k) + \text{Tr}(\mathbf{S}_k^* (\tilde{\mathbf{Q}}_{k+1} - \mathbf{Q}_k)).$$

We thus test the condition

$$J_\mu(\tilde{\mathbf{Q}}_{k+1}) < J_\mu(\mathbf{Q}_k) + \rho \text{Tr}(\mathbf{S}_k^* (\tilde{\mathbf{Q}}_{k+1} - \mathbf{Q}_k)), \quad (18)$$

for some parameter $\rho \in (0, 1)$. Typically, we take $\rho = 1/2$. If the condition (18) is met, we accept the candidate by setting $\mathbf{Q}_{k+1} = \tilde{\mathbf{Q}}_{k+1}$ and increase the step-size $\alpha_{k+1} = 2\alpha_k$. On the other hand, if the condition (18) fails, we discard the candidate by setting $\mathbf{Q}_{k+1} = \mathbf{Q}_k$ and decrease the step-size $\alpha_{k+1} = \alpha_k/2$.

C. Approximate ML Estimation via a GLM

The ISTA algorithm, Algorithm 1, is conceptually simple. But, the optimization may not be feasible for real-time implementations. The main challenge is the thresholding step $T_+(\cdot)$. Each thresholding step requires an eigenvalue decomposition. As we will see in the simulations, the algorithm often needs 100 iterations. The key insight is given by the following lemma:

Lemma 1: Given a set of measurement vectors \mathbf{u}_ℓ define the set

$$\mathbf{G} = \left\{ \mathbf{q} \mid \mathbf{Q} = \sum_{\ell=1}^L q_\ell \mathbf{u}_\ell \mathbf{u}_\ell^* + q_0 \mathbf{I} \geq 0 \right\}. \quad (19)$$

Then, the optimization (9) can be rewritten as an optimization over $\mathbf{q} \in \mathbf{G}$ via the equivalence

$$\min_{\mathbf{Q} \geq 0} J_\mu(\mathbf{Q}) = \min_{\mathbf{q} \in \mathbf{G}} f(\mathbf{A}\mathbf{q}), \quad (20)$$

where \mathbf{A} is the matrix with components

$$A_{\ell j} = \begin{cases} N & \text{if } j = 0, \ell = 0 \\ \|\mathbf{u}_j\|^2 & \text{if } j = 0, \ell > 0 \\ \|\mathbf{u}_\ell\|^2 & \text{if } \ell = 0, j > 0 \\ |\mathbf{u}_\ell^* \mathbf{u}_j|^2 & \text{if } j, \ell = 1, \dots, L, \end{cases} \quad (21)$$

and $f(\mathbf{z}) = \sum_{\ell=0}^L f_\ell(z_\ell)$, and

$$f_0(z_0) = \mu z_0 \quad (22a)$$

$$f_\ell(z_\ell) = \log \left(z_\ell + \frac{1}{\gamma} \|\mathbf{u}_\ell\|^2 \right) + \frac{y_\ell}{z_\ell + \frac{1}{\gamma} \|\mathbf{u}_\ell\|^2}, \quad \ell = 1, \dots, L. \quad (22b)$$

Proof: See Appendix A. \blacksquare

To understand the purpose of this lemma, recall that the chief computational difficulty in the ISTA algorithm arises from the thresholding step to impose the positivity constraint on $\mathbf{Q} \geq 0$. The above lemma shows that the optimization (9) over $N \times N$ matrices $\mathbf{Q} \geq 0$ can be replaced by an optimization over an $(L+1)$ -dimensional vector $\mathbf{q} \in \mathbf{G}$.

Unfortunately, the constraint in \mathbf{G} in (19) still requires a positivity constraint on the resulting matrix \mathbf{Q} . However, this problem can be approximately circumvented as follows: We know that if $\mathbf{q} > 0$ then

$$\mathbf{Q} = \sum_{\ell=1}^L q_\ell \mathbf{u}_\ell \mathbf{u}_\ell^* + q_0 \mathbf{I} \geq 0 \Rightarrow \mathbf{q} \in \mathbf{G}.$$

The converse is not true. That is, it is not the case that $\mathbf{q} \in \mathbf{G}$ implies that $\mathbf{q} \geq 0$. However, instead of searching over all $\mathbf{q} \in \mathbf{G}$, we can replace the optimization in (20) with the approximate ML optimization

$$\hat{\mathbf{q}} = \arg \min_{\mathbf{q} \geq 0} f(\mathbf{A}\mathbf{q}). \quad (23)$$

The resulting optimization (23) has a particularly simple structure. First, the vector \mathbf{q} has only componentwise constraints: $\mathbf{q} \geq 0$. Second, for any \mathbf{q} , the objective function

in (23) can be evaluated via a linear transform $\mathbf{z} = \mathbf{A}\mathbf{q}$ and followed by a sum of convex functions (22) on the components z_ℓ .

This type of optimization described by a separable function of a linear transform of the vector arises in a wide range of applications. The most common application is in inference problems for so-called generalized linear models (GLMs) [30].

D. An ISTA Algorithm for the Approximate ML

As before, we can apply an ISTA-type approach to the optimization (23) as follows. Let \mathbf{q}_k be the estimate at the k -th iteration and be its $\mathbf{z}_k = \mathbf{A}\mathbf{q}_k$ be its transform. We then find a $\alpha_k > 0$ such that,

$$f(\mathbf{A}\mathbf{q}) \leq \bar{f}(\mathbf{q}, \mathbf{q}_k) := f(\mathbf{A}\mathbf{q}_k) + \frac{\partial f(\mathbf{A}\mathbf{q}_k)}{\partial \mathbf{q}} \cdot (\mathbf{q} - \mathbf{q}_k) + \frac{1}{2\alpha_k} \|\mathbf{q} - \mathbf{q}_k\|_2^2, \quad (24)$$

for all possible $\mathbf{q} \geq 0$. So, $\bar{f}(\mathbf{q}, \mathbf{q}_k)$ is a quadratic upper bound on the true objective $f(\mathbf{A}\mathbf{q})$ that matches the true objective at the current estimate $\mathbf{q} = \mathbf{q}_k$. Also, the derivative in (24) is given by

$$\left. \frac{\partial f(\mathbf{A}\mathbf{q})}{\partial \mathbf{q}} \right|_{\mathbf{q}=\mathbf{q}_k} = \mathbf{s}_k^*, \quad \mathbf{s}_k := \mathbf{A}^* \frac{\partial f(\mathbf{z}_k)}{\partial \mathbf{z}}. \quad (25)$$

Then, as before, at each iteration k , the ISTA algorithm minimizes the upper bound $\bar{f}(\mathbf{q}, \mathbf{q}_k)$ instead of the true objective $f(\mathbf{A}\mathbf{q})$:

$$\begin{aligned} \mathbf{q}_{k+1} &= \arg \min_{\mathbf{q} \geq 0} \bar{f}(\mathbf{q}, \mathbf{q}_k) \\ &\stackrel{(a)}{=} \arg \min_{\mathbf{q} > 0} \mathbf{s}_k^* \mathbf{q} + \frac{1}{2\alpha_k} \|\mathbf{q} - \mathbf{q}_k\|_2^2 + \mu \mathbf{v}^T \mathbf{q} \\ &\stackrel{(b)}{=} \arg \min_{\mathbf{q} \geq 0} \|\mathbf{q} - \mathbf{q}_k + \alpha_k \mathbf{s}_k\|_2^2 + \mu \mathbf{v}^T \mathbf{q} \\ &\stackrel{(c)}{=} T_+(\mathbf{q}_k - \alpha_k \mathbf{s}_k), \end{aligned} \quad (26)$$

where in step (a) we substituted the definition of $\bar{f}(\cdot)$ in (24) and derivative (25) and removed terms that do not depend on \mathbf{q} ; step (b) follows from rearranging the quadratic and in step (c) the operator $T_+(\mathbf{p})$ is the proximal operator given by

$$T_+(\mathbf{p}) := \arg \min_{\mathbf{q} > 0} \|\mathbf{q} - \mathbf{p}\|_2^2. \quad (27)$$

which is simply the quadratic approximation and removing the negative components. It is easily checked that the proximal operator (27) is given by a simple thresholding operation

$$T_+(\mathbf{p}) := \max\{\mathbf{p}, 0\}, \quad (28)$$

which simply sets all negative components of \mathbf{p} to zero. The resulting algorithm is shown in Algorithm 2.

The main advantage of the Approximate ML algorithm, Algorithm 2 in comparison to Algorithm 1 is its complexity. Each iteration involves only multiplications by \mathbf{A} and \mathbf{A}^* as well as simple scalar derivatives. In particular, unlike Algorithm 1, there are no eigenvalue value decompositions needed for the thresholding step.

Algorithm 2 Approximate ML Estimation via ISTA

Require: Matrix search directions \mathbf{u}_ℓ and power values y_ℓ , $\ell = 1, \dots, L$, and SNR γ .

- 1: Construct \mathbf{A} in (21)
- 2: $k \leftarrow 0$
- 3: Initialize $\mathbf{q}_0 \geq 0$
- 4: **repeat**
- 5: $\mathbf{z}_k \leftarrow \mathbf{A}\mathbf{q}_k$
- 6: $\mathbf{s}_k \leftarrow \mathbf{A}^* \partial f(\mathbf{z}_k) / \partial \mathbf{z}$
- 7: Select step size $\alpha_k > 0$
- 8: $\mathbf{q}_{k+1} \leftarrow \max\{0, \mathbf{q}_k - \alpha_k \mathbf{s}_k\}$
- 9: **until** Terminated

Also, as with Algorithm 1, the objective function monotonically decreases with sufficiently small step-sizes α_k . Specifically, suppose that at some time k , α_k is sufficiently small that the bound (24) is satisfied for all \mathbf{q} . Then, we have

$$\bar{f}(\mathbf{q}_{k+1}) \stackrel{(a)}{\leq} \bar{f}(\mathbf{q}_{k+1}, \mathbf{q}_k) \stackrel{(b)}{\leq} \bar{f}(\mathbf{q}_k, \mathbf{q}_k) \stackrel{(c)}{=} f(\mathbf{q}_k), \quad (29)$$

where step (a) follows from quadratic upper bound approximation in (24), step (b) is based on monotonically decreasing behavior of the cost function when we are applying ISTA algorithm, and in step (c) we substituted the \mathbf{q}_k in (24). As in Section IV-B, we can adapt the step-size with a backtracking type rule.

V. NUMERICAL SIMULATION

A. Single-path Channel

To assess the performance of the proposed estimators, we first consider a theoretical single path channel. Specifically, we assume that, in each measurement ℓ and transmission d , the single-input multi-output (SIMO) channel is given by

$$\mathbf{h}_{\ell d} = \alpha_{\ell d} \mathbf{v}(\theta, \phi), \quad (30)$$

where θ and ϕ are the horizontal and vertical angles of arrival (AoAs) of the path, $\mathbf{v}(\theta, \phi)$ is the vector antenna response to the path, and $\alpha_{\ell d}$ is a complex scalar representing the small scale fading – see [33] for details. The parameters θ and ϕ are determined by the large-scale path directions and are thus assumed to be constant. However, we assume that the small-scale parameter $\alpha_{\ell d}$ is independently Rayleigh faded across different measurements ℓ and d . Under this single-path model, the average spatial covariance is then given by the rank one matrix

$$\mathbf{Q} = \mathbb{E}[\mathbf{h}_{\ell d} \mathbf{h}_{\ell d}^*] = \mathbb{E}|\alpha|^2 \mathbf{v}(\theta, \phi) \mathbf{v}^*(\theta, \phi). \quad (31)$$

We assume the power is normalized so that $\mathbb{E}|\alpha|^2 = 1$. Following [9], we assume a two-dimensional $4 \times 4 \lambda/2$ uniform linear array. This array size can be easily accommodated in a mobile in the mmW range. For example, at 28 GHz, the array would be only approximately 1.5 cm^2 . We set the SNR to 10 dB per antenna.

We then simulate the algorithm through 1000 Monte Carlo trials. In each trial, we generate random AoAs (θ, ϕ) and

random search directions \mathbf{u}_ℓ for the L measurements. The number of measurements L is varied. The random search directions \mathbf{u}_ℓ are taken as the antenna response along random angles that are generated in an i.i.d. manner. Following [32], we also take the diversity order $D = 4$. We then run the ML and approximate ML algorithm to compute estimates $\hat{\mathbf{Q}}$ of the true spatial covariance matrix \mathbf{Q} .

To evaluate the accuracy of the estimate $\hat{\mathbf{Q}}$, we measure the loss in beamforming resulting from the estimation errors. In general, given the true spatial covariance matrix \mathbf{Q} , the optimal long-term beamforming vector \mathbf{w}_{opt} is the unit vector directed along the maximal eigenvector of \mathbf{Q} . The optimal long-term beamforming gain is then

$$G_{opt} := \mathbf{w}_{opt}^* \mathbf{Q} \mathbf{w}_{opt} = \lambda_{max}(\mathbf{Q}),$$

where $\lambda_{max}(\mathbf{Q})$ is the maximal eigenvalue of \mathbf{Q} . For a rank-one single-path channel, the optimal beamforming vector is simply the vector aligned to the receive spatial signature, $\mathbf{w}_{opt} \propto \mathbf{v}(\theta, \phi)$. Also, assuming the spatial covariance matrix is normalized to unity $\text{Tr}(\mathbf{Q}) = 1$, the optimal beamforming gain is simply N , the dimension of the antenna array. See [10] for details.

To evaluate the loss from channel estimation errors, we suppose that the receiver applies a beamforming gain from the estimated covariance matrix $\hat{\mathbf{Q}}$. That is, we compute $\hat{\mathbf{w}}$ from the maximal eigenvector of $\hat{\mathbf{Q}}$ and then compute the actual gain,

$$G := \hat{\mathbf{w}}^* \mathbf{Q} \hat{\mathbf{w}}.$$

The loss is then given by

$$\text{loss} = 10 \log_{10}(G_{opt}/G),$$

which is the loss (in dB) due to the channel estimation error.

Fig. 3 plots the mean value of the loss as a function of the number of measurements L . There are several points to observe. First, we observe that with L around 60 measurements, the exact ML algorithm obtains a loss of less than 0.5 dB. Second, it should be pointed out that since the antenna array has dimension $N = 16$, the Hermitian matrix \mathbf{Q} has $N(N+1)/2 = 136$ unknowns. Hence, the low-rank method is successful in estimating the matrix well even though the number of measurements is below the number of free parameters. This property is precisely the value of the non-negative constraints. Third, the approximate ML method is only slightly inferior to the exact method. As mentioned above, the approximate ML method is significantly simpler to implement and thus the small additional loss may justify its use.

Finally, as a point of comparison, Fig. 3, plots the beamforming gain from a simple algorithm based on selecting the beamforming direction that resulted in the maximum power. Interestingly, this simple and intuitive algorithm performs considerably worse than the proposed method. For example, at $L = 60$ measurements, the loss is 1.5 dB, about 1 dB worse than the proposed ML estimation method.

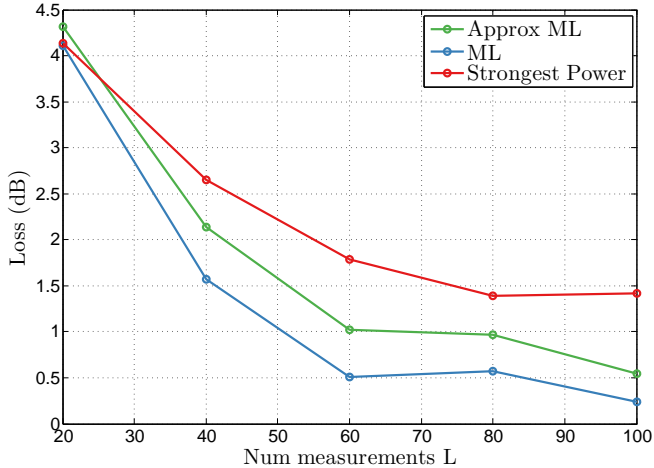


Fig. 3: Algorithm performance on a single-path channel. To estimate the performance of the algorithms, we computed the optimal beamforming vector for the estimated channel covariance matrix and then measured the loss in beamforming gain from applying the estimated vector relative to the optimal vector. The loss is plotted as a function of the number of power measurements L for different estimation algorithms assuming an ideal single path channel and a per antenna SNR of 10 dB.

B. Multi-path Channel using NYC Measurements

An important and surprising finding of the mmW measurements in New York City reported in [4], [16], [17] is that in urban micro-cellular type deployments, mmW signals are likely to propagate via multiple paths to the receiver. Although mmW signals are blocked by many materials, many street-level locations were able to see base stations at 100 to 200m via diffuse scattering and reflections, even when situated in non-line-of-sight (NLOS) locations. It is precisely this phenomena that enables mmW pico and micro-cellular type deployments.

To validate the channel estimation algorithms in these scenarios, we next simulated the algorithms with the spatial covariance matrix \mathbf{Q} generated from the model [9] derived from the New York City measurements [4], [16], [17] made at 28 GHz. The model in [9] follows a similar form to the standard 3GPP / ITU model [37], [38] with parameters fit to the mmW measurements. Specifically, the channel is composed of a random number of clusters, each cluster having some random angular spread and power. Based on data analysis in [9], the mmW channel typically has one to three clusters with a small angular spread in each clusters. Details can be found in [9].

Fig. 4 plots the loss for different number of directions, $L \in \{20, 60, 80, 100\}$. In comparison to the single path case, we see we need slightly more measurements. For example, for a 0.5 dB loss, we need $L = 100$ measurements. This number is still less than the number of free parameters. However, the other features remain the same. Specifically, the approximate ML results in only a small loss relative to the exact ML and both methods are considerably better than the simple strongest power method.

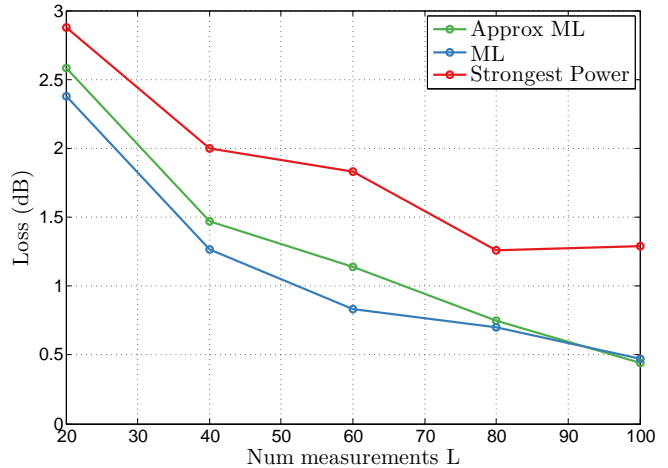


Fig. 4: Algorithm performance on a realistic multi-path channel. Details are identical to Fig. 3 except we use a multi-path channel model from [9] based on the real NYC measurements at 28 GHz [4].

C. Tuning the sparsity factor μ

In the simulations up to now, we have set the sparsity regularization parameter $\mu = 0$. That is, we have used the unregularized ML objective (8) instead of the regularized objective (10). However, given the low-rank nature of the channel, one may expect that adding a regularization term to force sparsity in the singular values of \mathbf{Q} would improve the estimation. To test this hypothesis, we evaluated the beamforming loss as a function of μ . Fig. 5 shows the average beamforming loss at $L = 50$ measurements as a function of the iteration number for three different values of μ . It can be seen that using a non-zero value of μ only makes the performance worse. Similar results were found at different values of L as well. Also, for the multipath channel, using $\mu > 0$ was even worse since the channel is inherently higher rank.

As described in Section III-C, the fact that $\mu = 0$ is optimal is not entirely surprising. The optimization (7) already imposes the positivity constraint $\mathbf{Q} \geq \mathbf{0}$. Similar to [35], non-negative constraints tend to naturally impose sparsity, so it is possible that additional sparsity regularization is not necessary.

CONCLUSIONS

Millimeter wave systems rely centrally on directional transmissions. Due to the rapid variations in the channel and need for low-latency communication, algorithms for fast spatial channels will thus be key for the successful deployment of these technologies. In this work, we have considered the estimation of the long-term receiver-side spatial covariance of the channel from analog beamformed power measurements. ML estimation is shown to be equivalent to an optimization that appears as a noisy, non-negative matrix completion problems. Fast algorithms were developed to solve this optimization and were demonstrated on both ideal single path channels as well as channel models derived from real measurements in urban deployments. The algorithms show relatively fast convergence

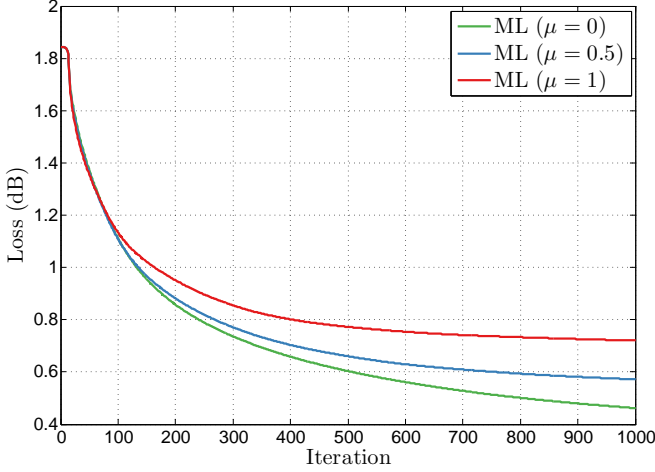


Fig. 5: Calculated loss for single path channel versus iterations that ISTA has been run for 50 different beamforming directions and different sparsity factors, $\mu = \{0, 0.5, 1\}$

(100 iterations) and can provide good tracking with significantly less number of measurements than unknowns.

Several future avenues of work are possible. First, we have considered only analog beamforming. Low-bit, fully digital, as proposed in [39], [40], may offer significantly improved performance and should be investigated. Also, the current algorithm assumes the long-term statistics are constant. Future work may also consider tracking of these parameters. Finally, the number of iterations for convergence is still somewhat long. Other approaches including Fast ISTA [41] and approximate message passing methods [42] may also be considered.

APPENDIX

PROOF OF LEMMA 1

First, we show that

$$\min_{\mathbf{Q} \geq \mathbf{0}} J_\mu(\mathbf{Q}) = \min_{\mathbf{Q} \in \mathbf{G}} J_\mu(\mathbf{Q}). \quad (32)$$

Since \mathbf{G} in (19) consists of positive matrices, we know that the left-hand side of (32) is less than or equal to the right-hand side. Hence, we need to show that the right-hand side is less than or equal to the left-hand side. To prove this, we need to show the following: For any $\mathbf{Q} \geq \mathbf{0}$, there exists a $\mathbf{Q}_0 \in \mathbf{G}$ with $J_\mu(\mathbf{Q}_0) = J_\mu(\mathbf{Q})$. Thus, let $\mathbf{Q} \geq \mathbf{0}$. Decompose \mathbf{Q} as

$$\mathbf{Q} = \mathbf{Q}_0 + \mathbf{R},$$

where $\mathbf{Q}_0 \in \mathbf{G}$ and $\mathbf{R} \perp \mathbf{G}$, where the orthogonality is with respect to the standard inner product between matrices, $\mathbf{A} \cdot \mathbf{B} = \text{Tr}(\mathbf{A}^* \mathbf{B})$. Now, since $\mathbf{R} \perp \mathbf{G}$ we have

$$\begin{aligned} \mathbf{R} \perp \mathbf{I} &\Rightarrow \text{Tr}(\mathbf{R}) = 0, \\ \mathbf{R} \perp \mathbf{u}_\ell \mathbf{u}_\ell^* &\Rightarrow \mathbf{u}_\ell^* \mathbf{R} \mathbf{u}_\ell = 0. \end{aligned}$$

Also, since $\mathbf{Q}_0 \in \mathbf{G}$, we have that

$$\mathbf{Q}_0 = \sum_{\ell=1}^L q_\ell \mathbf{u}_\ell \mathbf{u}_\ell^* + q_0 \mathbf{I},$$

for some coefficients q . So we have,

$$\begin{aligned} \lambda_\ell(\mathbf{Q}) &= \mathbf{u}_\ell^* [\mathbf{Q}_0 + \mathbf{R} + \gamma^{-1} \mathbf{I}] \mathbf{u}_\ell \\ &= \mathbf{u}_\ell^* [\mathbf{Q}_0 + \gamma^{-1} \mathbf{I}] \mathbf{u}_\ell \quad (\mathbf{R} \perp \mathbf{u}_\ell \mathbf{u}_\ell^*) \\ &= \lambda_\ell(\mathbf{Q}_0) \end{aligned} \quad (33)$$

Hence, from (8), $J(\mathbf{Q}) = J(\mathbf{Q}_0)$. Also, since $\text{Tr}(\mathbf{R}) = 0$,

$$\text{Tr}(\mathbf{Q}) = \text{Tr}(\mathbf{Q}_0 + \mathbf{R}) = \text{Tr}(\mathbf{Q}_0). \quad (34)$$

Therefore, from (10), $J_\mu(\mathbf{Q}) = J_\mu(\mathbf{Q}_0)$. Hence, for any $\mathbf{Q} \geq \mathbf{0}$, we can find a $\mathbf{Q}_0 \in \mathbf{G}$ with the same objective value $J_\mu(\mathbf{Q}) = J_\mu(\mathbf{Q}_0)$. This proves (32).

To prove (20), we need to show

$$J_\mu(\mathbf{Q}) = f(\mathbf{A}\mathbf{q}), \quad (35)$$

whenever \mathbf{Q} is of the form

$$\mathbf{Q} = \sum_{\ell=1}^L q_\ell \mathbf{u}_\ell \mathbf{u}_\ell^* + q_0 \mathbf{I}. \quad (36)$$

Let $\mathbf{z} = \mathbf{A}\mathbf{q}$. First observe that

$$\begin{aligned} \lambda_\ell(\mathbf{Q}) &\stackrel{(a)}{=} \mathbf{u}_\ell^* (\mathbf{Q} + \gamma^{-1} \mathbf{I}) \mathbf{u}_\ell \\ &\stackrel{(b)}{=} \sum_{j=1}^L q_j |\mathbf{u}_j^* \mathbf{u}_\ell|^2 + (q_0 + \gamma^{-1}) \|\mathbf{u}_\ell\|^2 \\ &\stackrel{(c)}{=} \sum_{j=0}^L A_{\ell j} q_j + \gamma^{-1} \|\mathbf{u}_\ell\|^2 \stackrel{(d)}{=} z_\ell + \gamma^{-1} \|\mathbf{u}_\ell\|^2, \end{aligned} \quad (37)$$

where (a) follows from (5), (b) follows from (36), (c) follows from the definition of the matrix components in (21) and (d) follows from the fact that $z_\ell = (\mathbf{A}\mathbf{q})_\ell$. Hence, the objective function $J(\mathbf{Q})$ in (8) is given by

$$\begin{aligned} J(\mathbf{Q}) &= \sum_{\ell=1}^L \log \left[z_\ell + \frac{1}{\gamma} \|\mathbf{u}_\ell\|^2 \right] + \frac{y_\ell}{z_\ell + \frac{1}{\gamma} \|\mathbf{u}_\ell\|^2} \\ &= \sum_{\ell=1}^L f_\ell(z_\ell), \end{aligned} \quad (38)$$

where the last step follows from (22). Also using (36),

$$\begin{aligned} \text{Tr}(\mathbf{Q}) &= Nq_0 + \sum_{j=1}^L q_j \|\mathbf{u}_j\|^2 \\ &\stackrel{(a)}{=} \sum_{j=0}^L A_{0j} q_j = z_0, \end{aligned} \quad (39)$$

where in (a) we again used (21). Hence, from (22),

$$\mu \text{Tr}(\mathbf{Q}) = f_0(z_0). \quad (40)$$

Combining (10), (38) and (40), we see that

$$J_\mu(\mathbf{Q}) = \sum_{\ell=0}^L f_\ell(z_\ell) = f(\mathbf{A}\mathbf{q}). \quad (41)$$

This proves (35) and the proof is complete.

REFERENCES

- [1] Cisco, "Cisco Visual Network Index: Global mobile traffic forecast update," 2013.
- [2] F. Khan and Z. Pi, "An introduction to millimeter-wave mobile broadband systems," *IEEE Comm. Mag.*, vol. 49, no. 6, pp. 101–107, Jun. 2011.
- [3] P. Pietraski, D. Britz, A. Roy, R. Pragada, and G. Charlton, "Millimeter wave and terahertz communications: Feasibility and challenges," *ZTE Communications*, vol. 10, no. 4, pp. 3–12, Dec. 2012.
- [4] T. S. Rappaport, S. Sun, R. Mayzus, H. Zhao, Y. Azar, K. Wang, G. N. Wong, J. K. Schulz, M. Samimi, and F. Gutierrez, "Millimeter Wave Mobile Communications for 5G Cellular: It Will Work!" *IEEE Access*, vol. 1, pp. 335–349, May 2013.
- [5] S. Rangan, T. S. Rappaport, and E. Erkip, "Millimeter-wave cellular wireless networks: Potentials and challenges," *Proceedings of the IEEE*, vol. 102, no. 3, pp. 366–385, March 2014.
- [6] F. Boccardi, R. W. Heath, A. Lozano, T. L. Marzetta, and P. Popovski, "Five disruptive technology directions for 5G," to appear in *IEEE Comm. Magazine*, 2014.
- [7] T. S. Rappaport, R. W. Heath Jr., R. C. Daniels, and J. N. Murdock, *Millimeter Wave Wireless Communications*. Pearson Education, 2014.
- [8] T. S. Rappaport, *Wireless Communications: Principles and Practice*, 2nd ed. Upper Saddle River, NJ: Prentice Hall, 2002.
- [9] M. Akdeniz, Y. Liu, M. Samimi, S. Sun, S. Rangan, T. Rappaport, and E. Erkip, "Millimeter wave channel modeling and cellular capacity evaluation," *IEEE J. Sel. Areas Comm.*, vol. 32, no. 6, pp. 1164–1179, June 2014.
- [10] A. Lozano, "Long-term transmit beamforming for wireless multicasting," in *Proc. ICASSP*, vol. 3, 2007, pp. III–417–III–420.
- [11] F. Khan and Z. Pi, "Millimeter-wave Mobile Broadband (MMB): Unleashing 3-300GHz Spectrum," in *Proc. IEEE Sarnoff Symposium*, Mar. 2011.
- [12] K.-J. Koh and G. M. Rebeiz, "0.13- m CMOS phase shifters for X-, Ku- and K-band phased arrays," *IEEE J. Solid-State Circuits*, vol. 42, no. 11, pp. 2535–2546, Nov. 2007.
- [13] —, "A Millimeter-Wave (4045 GHz) 16-Element Phased-Array Transmitter in a 0.18- μ m SiGe BiCMOS Technology," *IEEE J. Solid-State Circuits*, vol. 44, no. 5, pp. 1498–1509, May 2009.
- [14] X. Guan, H. Hashemi, and A. Hajimiri, "A fully integrated 24-GHz eight-element phased-array receiver in silicon," *IEEE J. Solid-State Circuits*, vol. 39, no. 12, pp. 2311–2320, Dec. 2004.
- [15] A. Alkhateeb, O. E. Ayach, G. Leus, and J. Robert W. Heath, "Hybrid analog-digital beamforming design for millimeter wave cellular systems with partial channel knowledge," in *Proc. Information Theory and Applications Workshop (ITA)*, Feb. 2013.
- [16] Y. Azar, G. N. Wong, K. Wang, R. Mayzus, J. K. Schulz, H. Zhao, F. Gutierrez, D. Hwang, and T. S. Rappaport, "28 GHz propagation measurements for outdoor cellular communications using steerable beam antennas in New York City," in *Proc. IEEE ICC*, 2013.
- [17] M. Samimi, K. Wang, Y. Azar, G. N. Wong, R. Mayzus, H. Zhao, J. K. Schulz, S. Sun, F. Gutierrez, and T. S. Rappaport, "28 GHz angle of arrival and angle of departure analysis for outdoor cellular communications using steerable beam antennas in New York City," in *Proc. IEEE VTC*, 2013.
- [18] A. F. Molisch and F. Tufevsson, "Propagation channel models for next-generation wireless communications systems," *IEICE Trans. Communications*, vol. 97, no. 10, pp. 2022–2034, 2014.
- [19] M. Martone, "An adaptive algorithm for antenna array low-rank processing in cellular TDMA base stations," *IEEE Trans. Communications*, vol. 46, no. 5, pp. 627–643, 1998.
- [20] B. Ottersten, "Array processing for wireless communications," in *Proc. IEEE Signal Processing Workshop on Statistical Signal and Array Processing*. IEEE, 1996, pp. 466–473.
- [21] X. Wang and H. V. Poor, "Blind multiuser detection: A subspace approach," *IEEE Trans. Information Theory*, vol. 44, no. 2, pp. 677–690, 1998.
- [22] J. Wright, A. Ganesh, S. Rao, Y. Peng, and Y. Ma, "Robust principal component analysis: Exact recovery of corrupted low-rank matrices via convex optimization," in *Proc. NIPS*, 2009, pp. 2080–2088.
- [23] Z. Lin, M. Chen, and Y. Ma, "The augmented lagrange multiplier method for exact recovery of corrupted low-rank matrices," *arXiv preprint arXiv:1009.5055*, 2010.
- [24] V. Koltchinskii, K. Lounici, A. B. Tsybakov *et al.*, "Nuclear-norm penalization and optimal rates for noisy low-rank matrix completion," *Annals of Statistics*, vol. 39, no. 5, pp. 2302–2329, 2011.
- [25] R. H. Keshavan, A. Montanari, and S. Oh, "Matrix completion from a few entries," *Information Theory, IEEE Transactions on*, vol. 56, no. 6, pp. 2980–2998, 2010.
- [26] S. Rangan and A. K. Fletcher, "Iterative estimation of constrained rank-one matrices in noise," in *Proc. IEEE ISIT*, 2012, pp. 1246–1250.
- [27] Y. Chen, Y. Chi, and A. J. Goldsmith, "Robust and universal covariance estimation from quadratic measurements via convex programming," in *Proc. ISIT*, Honolulu, HI, July 2014.
- [28] A. Beck and M. Teboulle, "A fast iterative shrinkage-thresholding algorithm for linear inverse problem," *SIAM J. Imag. Sci.*, vol. 2, no. 1, pp. 183–202, 2009.
- [29] J.-F. Cai, E. J. Candès, and Z. Shen, "A singular value thresholding algorithm for matrix completion," *SIAM Journal on Optimization*, vol. 20, no. 4, pp. 1956–1982, 2010.
- [30] J. A. Nelder and R. W. M. Wedderburn, "Generalized linear models," *J. Royal Stat. Soc. Series A*, vol. 135, pp. 370–385, 1972.
- [31] H. Zhao, R. Mayzus, S. Sun, M. Samimi, J. K. Schulz, Y. Azar, K. Wang, G. N. Wong, F. Gutierrez, and T. S. Rappaport, "28 GHz millimeter wave cellular communication measurements for reflection and penetration loss in and around buildings in New York City," in *Proc. IEEE ICC*, 2013.
- [32] C. N. Barati, S. A. Hosseini, S. Rangan, P. Liu, T. Korakis, and S. S. Panwar, "Directional cell search for millimeter wave cellular systems," *arXiv preprint arXiv:1404.5068*, 2014.
- [33] D. Tse and P. Viswanath, *Fundamentals of Wireless Communication*. Cambridge University Press, 2007.
- [34] D.-S. Shiu, G. J. Foschini, M. J. Gans, and J. M. Kahn, "Fading correlation and its effect on the capacity of multielement antenna systems," *IEEE Trans. Communications*, vol. 48, no. 3, pp. 502–513, 2000.
- [35] D. D. Lee and H. S. Seung, "Algorithms for non-negative matrix factorization," in *Proc. NIPS*, Dec. 2001, pp. 556–562.
- [36] J. Nocedal and S. J. Wright, "Numerical optimization," *Numerical optimization*, pp. 497–528, 2006.
- [37] 3GPP, "Further advancements for E-UTRA physical layer aspects," TR 36.814 (release 9), 2010.
- [38] ITU, "M.2134: Requirements related to technical performance for IMT-Advanced radio interfaces," Technical Report, 2009.
- [39] H. Zhang, S. Venkateswaran, and U. Madhow, "Analog multitone with interference suppression: Relieving the ADC bottleneck for wideband 60 GHz systems," in *Proc. IEEE Globecom*, Nov. 2012.
- [40] D. Ramasamy, S. Venkateswaran, and U. Madhow, "Compressive tracking with 1000-element arrays: a framework for multi-gbps mm wave cellular downlinks," in *Proc. 50th Ann. Allerton Conf. on Commun., Control and Comp.*, Monticello, IL, Sep. 2012.
- [41] Y. E. Nesterov, "Gradient methods for minimizing composite objective function," *CORE Report*, 2007.
- [42] S. Rangan, "Generalized approximate message passing for estimation with random linear mixing," in *Proc. IEEE Int. Symp. Inform. Theory*, Saint Petersburg, Russia, Jul.–Aug. 2011, pp. 2174–2178.